Electronic Supplementary Material (ESI) for Organic & Biomolecular Chemistry

Bound Water is Central to Both Molecular Recognition and Function in the Catalase Enzyme

*Marco Candelaresi[a], Andrea Gumiero[b], Katrin Adamczyk[a], Kirsty Robb[c], César Bellota-Antón[c], Vartul Sangal[c], John Munnoch[d], Gregory M. Greetham[e], Michael Towrie[e], Anthony W. Parker[e], Paul A. Hoskisson[c], Nicholas P. Tucker,[c] Martin A. Walsh[b] and Neil T. Hunt[a]**

[a]*Department of Physics, University of Strathclyde, 107 Rottenrow East, Glasgow, G4 0NG, United Kingdom,*

[b]*Diamond Light Source, Harwell Science and Innovation Campus, Didcot, OX11 0QX, United Kingdom*

[c]*Strathclyde Institute of Pharmacy and Biomedical Sciences, University of Strathclyde, 161 Cathedral Street, Glasgow, G4 0RE, United Kingdom,*

[d]*School of Biological Sciences, University of East Anglia, Norwich, NR4 7TJ, United Kingdom,*

[e]*Central Laser Facility, Research Complex at Harwell, Rutherford Appleton Laboratory, Didcot, OX11 0QX, United Kingdom*

Correspondence email: neil.hunt@strath.ac.uk

SUPPORTING INFORMATION

Biochemistry:

The *in vitro* turnover rate of H_2O_2 by *C. glutamicum* catalase was measured and the results are shown in Fig 1A (main text). Fitting of the pseudo-linear portion of the data ($[H_2O_2]$ < 30mM) to the Michaelis-Menten model:

$$V = \frac{V_{\max}[S]}{[S] + K_m}$$

where V denotes the rate of reaction, [S] the substrate (H_2O_2) concentration, V_{max} the maximum rate and K_m the Michaelis constant, was carried out. The results of this process are given in the main text and, based on this observation, subsequent peroxidase assays were performed at substrate concentrations of 25 mM.

Whole organism biology:

Cultures of *C. glutamicum* and the *C. glutamicum katA* mutant were grown to the mid-exponential growth phase (1 x 10^8 CFU/ml) and then treated with a final concentration of 1 % H_2O_2 to assess survival or pre-treated for 30 mins with MAHMA-NONOate (0.002 M final concentration) before exposing to 1 % H_2O_2 (Main text Fig. 1A).

Following treatment with H_2O_2 wild type *C. glutamicum* continue to grow, probably reflecting the level of intrinsic expression of *katA* during aerobic growth and thus are clearly able to resist the effects of H_2O_2 (Main text, Fig. 1D, filled squares). By contrast, pre-treatment with MAHMA-NONOate resulted in only 20% survival after 60 minutes (Fig. 1D, filled circles). No effect on the growth rate was observed when the cells were treated with NO alone.

Repeating the experiment with a *katA* mutant strain resulted in reduced resistance to H_2O_2 treatment, with 100 % of the mutant cells being dead within 60 minutes of the addition of H_2O_2 (Fig. 1D, filled triangles). The pre-treatment of the *katA* mutant with MAHMA-NONOate prior to the addition of H_2O_2 resulted in complete death of the cultures within 30 minutes of the treatment (Fig. 1D, open triangles).

X-ray Crystallography:

The UV-vis spectroscopy of the crystalline form of catalase was consistent with that in solution. Upon treatment with nitric oxide (NO), the spectrum of the crystals was observed to undergo a change with peaks at 501 nm, 538 nm and 622 nm (Fig. S1A, dashed line) being replaced by peaks at 540 nm and 577 nm (Fig. S1A, solid line). This is consistent with a 5 or 6-coordinate high spin state in the native enzyme becoming a 6 coordinate low spin species, as would be expected upon formation of an NO-complex.

The impact of X-ray photoreduction on the catalase crystals was assessed by observing the decrease in the difference of absorbance between the peak at 577 nm and the trough at 558 nm as a function of X-ray dose (Fig. S1B, arrows). It was estimated that a dose of approximately 0.5 MGy (calculated with RADDOSE [1]) results in a 20% reduction of the ferric haem in the small region of the crystal that was irradiated. Thus, in order to limit photoreduction, a line-scan diffraction strategy was applied and diffraction images were collected by using an X-ray micro-beam (20 x 20 μm) and exposing 10 contiguous sections of the crystals, each for a maximum dose of 0.5 MGy [1].

X-ray crystallographic data and refinement statistics for the structures obtained are given in Table S1 below.

Table S1. *Crystallographic data and refinement statistics.*

Protein	**Cat**	**Cat-NO**
PDB	4b7g	4b7f
Space group	$P6_3$	$P6_3$
Cell dimensions		
a, b, c (Å)	151.75 151.75 157.68	151.51 151.51 156.62
α, β, γ (°)	90 90 120	90 90 120
Resolution	50.0 - 1.90 (1.92 - 1.90)	100 – 1.76 (1.81 – 1.76)
R_{merge} (%)	11.8 (66.5)	9.9 (59.3)
I/σI	7.0 (1.8)	9.0 (2.4)
Completeness (%)	99.6 (95.2)	93.4 (93.6)
Redundancy	6.7 (4.2)	3.7 (3.7)
Refinement		
No. reflections	160649	177534
R_{work}/R_{free} (%)	13.30 / 17.43	12.99 /16.64
No. atoms		
Protein	16687	17036
Water	2343	2328
Ligands/Ions	462	420
R.m.s. deviations		
Bond lengths (Å)	0.008	0.016
Bond angles (Å)	1.183	1.729

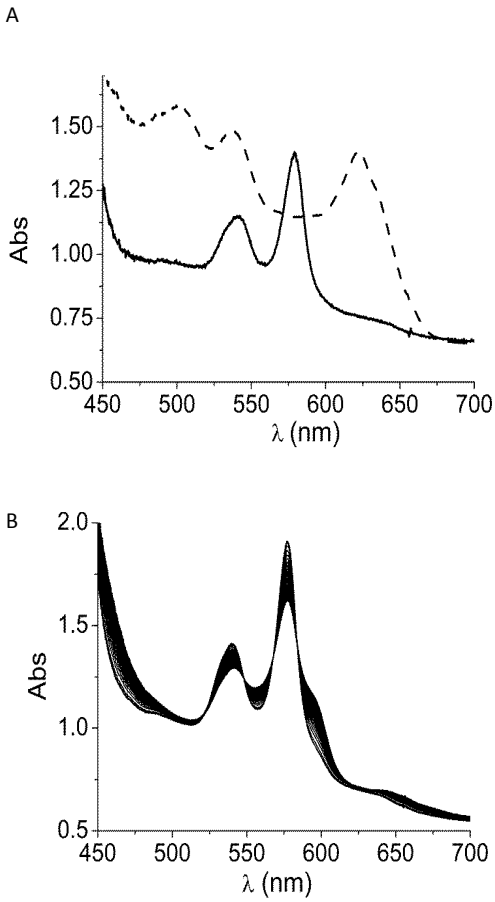

Fig S1: *Single crystal UV-vis absorbance spectrum of crystals of catalase from corynebacterium glutamicum at 100 K. A) Solid line: Catalase-NO, peaks at 540 nm and 577 nm. Dashed line: native enzyme, peaks at 501 nm, 538 nm and 622 nm. B) Superimposition of 70 spectra collected during X-ray exposure, between 0 and 2.0 MGy, showing the change of the spectrum due to photoreduction. Arrows indicate the spectral changes arising from the decay.*

Infrared and 2D-IR Spectroscopy:

The FTIR spectrum of nitrosylated catalase is shown in Fig. S2. This peak was well-reproduced by fitting to a single Gaussian profile centred at 1881 cm^{-1} with a full width half maximum of 7 cm^{-1}, consistent with the presence of a single conformational form for catalase-NO under these conditions. The results of the fit are shown in Fig. S2. It is noted that ferric-NO complexes are known to undergo auto reduction on timescales of a few hours, however, no evidence for loss of the ferric form was observed during FTIR or 2D-IR data collection and it is noted that experiments exploiting the ν_{NO} IR transition near 1900 cm^{-1} are uniquely sensitive to the ferric form of the complex.

2D-IR data fitting:

The 2D-IR spectra such as those shown in Fig. 4A-C (main text) were fit to a 2D Gaussian lineshape function of the form:

$$\sum_i A_i \exp\left[-\frac{1}{2(1-C_{2D,i}^2)}\left[\left(\frac{x-x_{0,i}}{\sigma_{x,i}}\right)^2+\left(\frac{y-y_{0,i}}{\sigma_{y,i}}\right)^2-\frac{2C_{2D,i}(x-x_{0,i})(y-y_{0,i})}{\sigma_{x,i}\sigma_{y,i}}\right]\right]$$

where A is the amplitude, x_0 and y_0 are the central frequencies in the ω_{probe} and ω_{pump} directions respectively, and the σ_x and σ_y are the widths along these axes. In equation 1, C_{2D} represents a cross-correlation parameter, which takes values from -1 to 1 and provides a measure of the diagonal elongation of the 2D-IR peak shape. A C_{2D} value of 1 represents a strong correlation between the pump and probe frequencies and so an elongated lineshape. As the correlation is reduced C_{2D} approaches 0 and the 2D lineshape becomes more circular. A value of -1 indicates an anticorrelated lineshape.

The temporal dependence of the C_{2D} parameter (Fig. 5, main text) was subsequently fit to an exponential decay function of the form:

$$C_{2D} = a_1 \exp\left(\frac{-t}{\tau}\right) + a_c$$

where a_1 represents the amplitude, τ is the decay time and a_c is a constant (pseudo-static) term that effectively represents the contribution from decay processes that are slow on the timescale of the experiment.

Using infrared pump-probe spectroscopy, the vibrational relaxation time of the NO stretching vibration of catalase was observed to be 16 ps.

DISCUSSION

Crystallography data shows that the NO ligand binds to catalase-NO in a bent geometry with an angle of around 30° with respect to the normal of the haem plane. This value is greater than that reported for bovine liver catalase,[2] but the value was found to be strongly model-dependent. A bent NO geometry is somewhat contradictory to the established view of Fe^{III}-NO, which is expected to yield a linear Fe-N-O moiety in accordance with the isoelectronic nature of the Fe^{II}-NO^+ ground state with that of Fe^{II}-CO.[3] While this might indicate a ferrous contribution to the binding of NO, it is clear from the IR absorption frequency and the UV-vis spectra that the system is ferric in character. Spectroscopy experiments[4] and DFT calculations[5] are also in agreement with a bent NO binding geometry. In particular, a study of ferric Mb-NO via time-resolved IR spectroscopy determined the angle between the dipole moment of NO and the normal to the haem plane to be 22.7°, which is consistent with our results and was ascribed to an interaction between the lone pair of the distal his64 and the nitrogen of the NO ligand.[4]

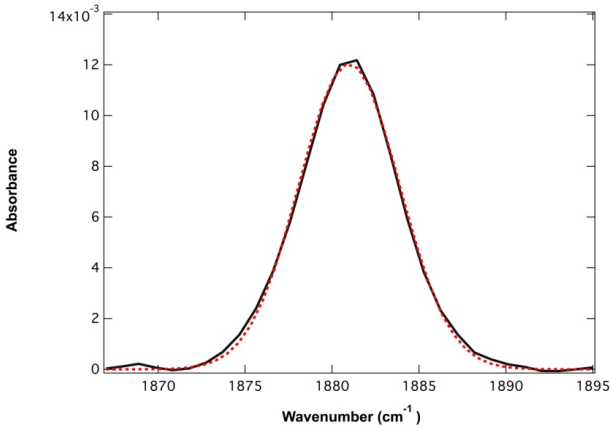

Fig S2: *FT-IR spectrum of catalase-NO near 1880 cm^{-1} (black). The red dashed line corresponds to the results of fitting to a Gaussian lineshape function (see text).*

REFERENCES

1 Paithankar, K. S., Owen, R. L., and Garman, E. F., *Absorbed dose calculations for macromolecular crystals: improvements to RADDOSE, J Synchrotron Radiat* **16**, 152 (2009).

2 Purwar, N. McGarry, J. M., Kostera, J., Pacheco, A. A. , Schmidt, M. *Interaction of Nitric Oxide with Catalase: Structural and Kinetic analysis, Biochemistry* **50**, 4491 (2011).
3 Nutt, D. R. and Meuwly, M., *Ferric and ferrous iron in nitroso-myoglobin: Computer simulations of stable and metastable states and their infrared spectra, ChemPhysChem* **8**, 527 (2007).
4 Zemojtel, T., Rini, M., Heyne, K., Dandekar, T., Nibbering, E. T. J., and Kozlowski, P. M., *No-Bound Myoglobin: Structural Diversity and Dynamics of the NO Ligand, J. Am. Chem. Soc.* **126**, 1930 (2004).
5 Soldatova, A. V., Ibrahim, M., Olson, J. S., Czernuszewicz, R. S., and Spiro, T. G., *New Light on NO Bonding in Fe(III) Heme Proteins from Resonance Raman Spectroscopy and DFT Modeling, J. Am. Chem. Soc.* **132**, 4614 (2010)